JOURNAL OF PROPULSION AND POWER
Vol. 23, No. 1, January–February 2007

Regression Rates Study of Mixed Hybrid Propellants

Robert A. Frederick Jr., J. Joshua Whitehead, L. Richard Knox, and Marlow D. Moser
University of Alabama in Huntsville Propulsion Research Center, Huntsville, Alabama 35899

DOI: 10.2514/1.14327

The low regression rates of classic hybrid rocket fuels lead to large internal ports that limit potential applications. This experimental study investigated the increase in regression rate that results from adding a solid oxidizer and a catalyst to a hybrid fuel grain. The configuration is named a "mixed hybrid" hybrid to signify solid oxidizer and catalyst in the grain. A design of experiments approach guided fuel formulation to systematically control levels of ammonium perchlorate from 25% to 30%, ferric oxide from 0 to 5%, and hydroxyl-terminated polybutadiene from 70% to 75%. The 1.5-in. diam. port, 12-in. long center perforated grains were burned with gaseous oxygen at pressure levels from 150 to 550 psig and port flux levels from 0.1 to 0.4 lbm/s-in.^{2}. The results show that the mixed hybrid propellants burn as a function of both pressure and mass flux. A grain formulation having 27.5% ammonium perchlorate and 2.5% ferric oxide provided the maximum burning rate augmentation (447%) among the formulations tested.

Nomenclature

a	=	regression rate law coefficient
C_d	=	venturi discharge coefficient
D	=	rocket aft nozzle diameter
D_f	=	calculated final solid propellant port diameter
D_i	=	initial solid propellant port diameter
D_{vent}	=	throat diameter of oxidizer feed system sonic venturi
Fe_2O_3	=	iron oxide (also referred to as catalyst or additive)
f	=	number of data points in pressure integral
G_{ox}	=	oxidizer mass flux, lb/s-in.^{2}
$\bar{G}_{\text{ox}}$	=	average oxidizer mass flux, lb/s-in.^{2}
L	=	length of propellant grain
L^*	=	characteristic chamber length
m	=	oxidizer mass flux exponent in regression rate law
m_f	=	final mass of propellant grain
m_i	=	initial mass of propellant grain
$\dot{m}_{\text{ox}}$	=	mass flow rate of oxidizer
n	=	pressure exponent in regression rate law
P	=	chamber pressure
P_{avg}	=	average chamber pressure
P_{up}	=	pressure upstream of venturi
R	=	specific gas constant
$\bar{\dot{r}}$	=	average regression rate of propellant grain
T_{up}	=	temperature upstream of venturi
t_b	=	burn time or difference between initial and final action time
t_f	=	final action time
t_i	=	initial action time
U_i	=	uncertainty in an independent variable x_i
x_i	=	measured variables in uncertainty analysis
γ	=	specific heat ratio
ρ_f	=	density of solid propellant grain

Introduction

HYBRID propulsion systems have been examined over the years to address the issues of safety and controllability that are difficult for solid propellants [1]. Separating the oxidizer and fuel increases safety. The flow of oxidizer controls the thrust. However, because of the inherent low burning rates of the solid fuels, new applications of hybrid systems are often limited by their poor volumetric loading.

There exists a relatively unexplored region of propellants that lie between the limits of a conventional solid propellant and a classic hybrid system. In this regime, the hybrid approach is still employed but low levels of oxidizers and catalyst are put into the solid fuel. This is now named a mixed hybrid system to refer to the mixing of solid oxidizer and catalyst in the solid fuel grain. In a mixed hybrid system, oxidizer flow is injected into a chamber lined with a mixed hybrid propellant.

Increasing the density and regression rate of the solid portion of this system results in a significant reduction in motor size as compared with conventional, inert hybrid-fueled grains. A past study has shown that with as little as a 10% increase in the regression rate over conventional hybrids, an upper stage can be shortened by 20% in length. This translates into lower cost. The ability to stop and restart provides mission flexibility, abort options, and broader applications of this propulsion system. Low levels of oxidizer could result in a decrease in hazards when compared with conventional solid propellants.

Past work has investigated various solid additives to increase the regression rates in hybrid rockets. A study with hydroxyl-terminated polybutadiene (HTPB) and 7.55% ammonium perchlorate (AP) hybrid fuel burned with gaseous oxygen at 2.0 MPa and an oxidizer flux of 450 kg/m^2-s showed some burning rate augmentation (up to 31% increase compared to pure HTPB) and no significant pressure sensitivity for the pressure ranges tested [2]. An addition of 19.67% aluminum provided an increase in regression rate of 85% at the same oxidizer flux. Grain profiles were also assessed after firing and showed that a general increase in port diameter was present axially from the head to the aft end of the grain. Effects of initial port diameter, fuel grain length, and the addition of AP and aluminum were investigated with respect to the regression rate of the solid fuel. Reduction of grain port diameter was found to be the most significant factor for the enhancement of the regression rate at similar flux levels. Chiaverini et al. [3] fired HTPB grains containing 20% activated aluminum with gaseous oxygen and found the regression rate to increase by 40% with respect to pure HTPB. In addition to studies involving HTPB-based fuels, experiments by De Zilwa et al [4]. were conducted with paraffin-based hybrid fuel grains fired with gaseous oxygen. Regression rates up to 300% that of HTPB-based hybrid fuels were observed.

The objective of this study is to experimentally determine the ballistic properties of mixed hybrid propellants and to determine if significant improvements in regression rate (and thereby increase mass flow per volume) are possible. This investigation evaluated the burning rate characteristics of HTPB (mixed with controlled

Presented as Paper 3824 at the 40th AIAA/ASME/SAE/ASEE Joint Propulsion Conference and Exhibit, Fort Lauderdale, Florida, 11–14 July 2004; received 26 January 2005; revision received 4 April 2006; accepted for publication 28 August 2006.

amounts of catalyst and AP) burning with gaseous oxygen. The resulting ballistic correlations show the effects of grain formulation, pressure, and mass flux on the solid grain burning rate. The results show that addition of these materials substantially augments the regression rate when compared to a pure hybrid while maintaining a stop–start capability. This research fills a relatively uncharted class of solid formulations that exists between solid and hybrid rocket technologies. The results are experimental burning rate laws for a systematic variation of formulation variables and test conditions in this regime. The test data in this article were partially presented in earlier papers [5,6] and now analyzed with a modified data reduction method.

Approach

Design of Study

The working hypothesis for this experimental study is that the mixed hybrid fuels respond to both the oxidizer mass flux through the port G_{ox} and the chamber pressure P. A solid propellant's burning rate is mainly dependent on the pressure while that of a hybrid fuel is dependent mainly on the oxidizer flux through the grain. A combination of these effects is proposed mathematically as

$$\dot{r} = aG_{ox}^{m}P^{n} \tag{1}$$

Three unknown coefficients a, m, and n must be experimentally determined. This required a minimum of three different sets of pressure/oxygen-flux operating conditions be tested for each propellant formulation.

The mixed hybrid grain formulations were designed with three components: HTPB, AP, and a catalyst. The first component was HTPB which is commonly used as a binder in solid rocket propellants. Burned without the other solid ingredients, it represents the classic hybrid cycle. The second component, AP, was added at levels from 25% to 30% to increase the burning rate and density of the grain. Although unproven, this range of AP level was hypothesized as an upper limit for extinguishment and 1.4 hazards classification. Two-micron diameter AP particles were chosen for use in the propellant. The third component was ferric oxide, a classical solid propellant burning rate catalyst, added at levels ranging from 0 to 5%. Formulations tested are tabulated in Table 1.

The propellant formulation matrix is designed based on the design of the experiments theory, which changes the ingredients in a systematic way [5]. Figure 1 shows the six propellant formulations plotted on a ternary diagram. The formulation points are selected based on requiring a 5% range of the three components and the points are distributed for a quadratic mixture study [5]. One pure fuel with 100% HTPB was also included in the study for comparison as a baseline. Grains were mandrel cast and cured in phenolic sleeves with a port initial diameter of 1.50 in., a length of 12.0 in., and a web thickness of 0.25 in.

Gaseous oxygen was used as the injected oxidizer and to provide results that apply to higher performance launch systems. The test conditions were designed to control both the flux and the pressure in the grain. The maximum and minimum values of initial $\bar{G}_{ox}$ have a 4:1 ratio and the range test pressures had a 2:1 ratio. A 4:1 pressure ratio was planned but nozzle erosion limited the higher pressures. High and low $\bar{G}_{ox}$ levels were targeted during experimentation at 0.4 and 0.1 lbm/in.^{2}-s, respectively. The $\bar{G}_{ox}$ ranges are consistent with

Table 1 Mixture formulations for assessment of mixed hybrid concept

Propellant mix	HTPB, wt %	AP, wt %	Fe_2O_3, wt %
A	72.5	27.5	0.0
B	72.5	25.0	2.5
C	70.0	27.5	2.5
D	75.0	25.0	0.0
E	70.0	30.0	0.0
F	70.0	25.0	5.0
HTPB	100.0	0.0	0.0

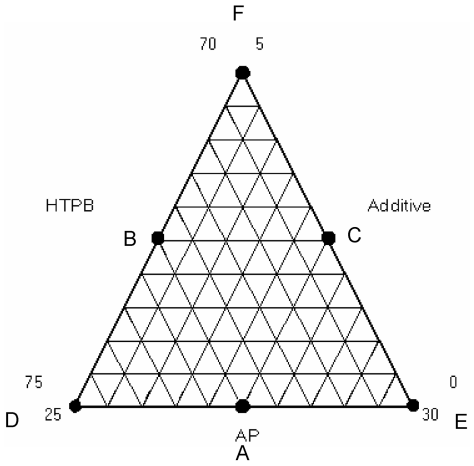

Fig. 1 Ternary mixture diagram for the assessment of the mixed hybrid concept.

test conditions from past research and are on the lower end of values that would be used in launch vehicles [6]. The pressure range is at the low end of the range for pressure-fed missiles but covers a sufficient span to estimate the pressure sensitivity ballistic properties. The flux is controlled by the oxidizer mass flow rate into the port and the port diameter. Therefore, burning the grain completely causes the G_{ox} level to decrease by about 46% during an experiment.

Table 2 shows the test matrix. Because the number of grains was limited, the endpoints of a wide span of pressures and fluxes were specified. Tests were designed to operate at pressures of 250 or 500 psig. Because the propellant ballistic properties were not known before the test, HTPB regression rate data guided the sizing of the nozzles to the target pressure levels.

Methods of Testing

The propulsion test facility provided the feed system and instrumentation for the testing. Instrumentation includes pressure, temperature, and thrust transducers to monitor flow rates and performance of the propulsion system. Video cameras monitor the test area for safety. Testing was conducted using a laboratory-scale motor assembly. A diagram of the experimental assembly is given in Fig. 2. The grains were cartridge loaded into a segment of machined steel tubing with 1/4 in. walls that acted as the outer protective layer of the combustion chamber. Head and aft ends of the motor were constructed using stainless steel. A phenolic entry section at the head end of the motor was machined to allow for smooth entrance of oxidizer flow into the combustion chamber and to provide some insulation from the high temperatures achieved during burning. Nozzles were machined from oxygen-free copper. Copper entry pieces were machined to insulate the copper nozzles and prevent throat erosion during testing.

The gaseous oxygen is delivered from six k bottles through a manifold. The main oxidizer flows through 3/4 in. tubing, and a dome loader regulates the pressure. The dome loader is charged by gaseous nitrogen and actuated by a three-way pneumatic ball valve. The mass flow rate of the oxidizer is managed with a sonic choke venturi. Just upstream of the venturi are a pressure transducer and a thermocouple enabling the mass flow rate of the gaseous oxygen to be accurately measured. Oxygen is delivered into the combustion chamber through a rearward facing dump injector.

Table 2 Target experimental operating conditions

Operating conditions	G_{ox}, lbm/in.^{2}-s	Chamber pressure, psi
High G_{ox}, low P	0.4	250
Low G_{ox}, high P	0.1	500
Low G_{ox}, low P	0.1	250

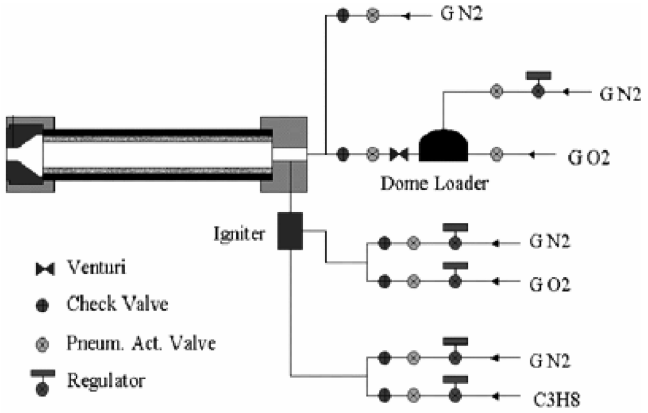

Fig. 2 Experimental motor assembly, feed lines, purge lines, and igniter.

An OMRON programmable logic controller (PLC) was used to activate all valves in a preprogrammed order for each test firing. Pressure and temperature sensors throughout the experimental apparatus were routed through the InstruNet-100 A/D (analog to digital) converter before being sent back to the control room for continuous review and recording. Data collection was controlled using Labview software in a remote control room. The Labview program operated at a data sampling frequency of 100 Hz. Data on selected runs were taken at 1000 hz to check for higher-frequency oscillations. In addition, an OHAUS 4000 × 0.1 g digital scale was used for all weight measurements.

A typical test sequence is presented in Table 3. Firing time was set based on the formulation and operating conditions used and varied up to a level of approximately 3 s. It should be noted in Table 3 that the G_{ox} and Igniter Purge being turned on does not indicate that nitrogen is flowing through the motor during the test. The purge lines

$$P_{avg} = \frac{\int_{t_i}^{t_f} P\,dt}{\int_{t_i}^{t_f} dt} \cong \frac{\sum_{j=i}^{f}[(\frac{P_{j+1}+P_j}{2})(t_{j+1}-t_j)]}{t_f - t_i} \tag{2}$$

Test data were also reduced to determine the average oxidizer mass flux and average regression rate of each run. The oxidizer mass flux was determined from the average temperature and pressure upstream of the venturi along with the initial and final masses of the fuel. This includes the assumption that average, initial, and final port diameters are determined by the mass change occurring during combustion:

$$\bar{G}_{ox} = \frac{\dot{m}_{ox}}{A_P} = \frac{2C_d \cdot P_{up} \cdot D_{vent}^2 \cdot \gamma \cdot \sqrt{[\frac{2}{\gamma+1}]^{\frac{\gamma+1}{\gamma-1}}}}{(\frac{4\cdot(m_i-m_f)}{\pi\cdot\rho_f\cdot L} + D_i^2)\cdot\sqrt{\gamma\cdot R\cdot T_{up}}} \tag{3}$$

where

$$\frac{4\cdot(m_i-m_f)}{\pi\cdot\rho_f\cdot L} = D_f^2 \tag{4}$$

To estimate a regression rate of the fuel, a time-averaged approach was used [7]. The mass consumption measured was assumed to occur evenly over the port surface area without burning on the ends of the grain. Initial and final mass of the propellant grain were determined and applied to find the average change in port radius that occurred

Table 3 Sequence of test operation. GOX = gaseous oxygen

Action	Timeline, s
Propane on	0.10
GOX igniter on	0.20
Spark on	0.20
Spark off	0.60
Main GOX on	0.70
GOX igniter purge on	0.90
Propane igniter purge on	0.90
GOX igniter off	1.20
Propane off	1.20
Main GOX purge on	2.00
Main GOX off	3.70
GOX igniter purge off	10.90
Propane igniter purge off	10.90
Main GOX purge off	12.00

are situated behind check valves and set to pressure levels of about 50 psi. This means that the purge will not flow until the motor chamber pressure drops below 50 psi. This strategy allows the purges to automatically come on at the end of the test or in the event of a failure rather than waiting on a preprogrammed time. Likewise, the flow of igniter propane and igniter oxygen is automatically stopped as the motor pressure exceeds their supply pressure. Extended duration (greater than 5 s) burns were initially tried but lead to significant nozzle erosion. Additionally, burn times for faster burning grains (those containing oxidizer and catalyst) were shorter to ensure that all propellant was not consumed.

Reduction of Data

To relate experimental data to the proposed regression rate law [Eq. (1)], average pressure and oxidizer flux were calculated for each experimental run. Average pressure was calculated by application of the trapezoid rule for numerical integration.
during the burn.

$$\bar{\dot{r}} \approx \frac{\Delta r}{\Delta t} = \frac{\sqrt{4(m_i - m_f)/\pi\rho_f L + D_i^2} - D_i}{2(t_f - t_i)} \tag{5}$$

Initial and final action times were assessed at the time of interception of a constant pressure line on the pressure-time trace at 50% of the maximum pressure achieved during the burn. The difference between these initial and final action times was defined as the burn time for the test as used in Eq. (5).

A generalized uncertainty analysis estimate was done following the accepted methods of Coleman and Steele [8], more specifically the propagation equation method. The propagation equation method is a way to observe how the uncertainties of the individual measured variables propagate into the formulation of the result. A detailed process of the use of the propagation equation method for a laboratory-scale hybrid rocket motor has been done previously by Greiner and Frederick [9]. For purposes of calculation, the systematic uncertainties are assumed to be small in comparison with the random ones. The impact of uncertainties in each of the measured variables is used to determine the uncertainty of the calculated value:

$$U_r = \sqrt{\left(\frac{\partial\bar{\dot{r}}}{\partial m_i}\cdot U_{m_i}\right)^2 + \left(\frac{\partial\bar{\dot{r}}}{\partial m_f}\cdot U_{m_f}\right)^2 + \left(\frac{\partial\bar{\dot{r}}}{\partial D_i}\cdot U_{D_i}\right)^2 + \left(\frac{\partial\bar{\dot{r}}}{\partial \rho_f}\cdot U_{\rho_f}\right)^2 + \left(\frac{\partial\bar{\dot{r}}}{\partial L}\cdot U_L\right)^2 + \left(\frac{\partial\bar{\dot{r}}}{\partial t_b}\cdot U_{t_b}\right)^2} \tag{6}$$

Table 4 Measurement uncertainties for regression rate calculation

Measured value	Symbol	Uncertainty	Units
Initial propellant mass	m_i	0.10	g
Final propellant mass	m_f	0.10	g
Initial port diameter	D_i	0.05	in.
Fuel grain density	ρ_f	0.01	g/cm^3
Combustion chamber length	L	0.05	in.
Burning time	t_b	0.10	s

Individual contributions of each independent variable are determined by calculation of the partial derivative of the calculated function with respect to the measured quantity. As an example, the contribution to regression rate from initial port diameter is given in Eq. (7),

$$\frac{\partial \dot{r}}{\partial D_i} = \frac{D_i}{2t_b} \cdot \left(\frac{4(m_i - m_f)}{\pi \rho_f L} + D_i^2 \right)^{-0.5} - \frac{1}{2t_b} \tag{7}$$

Measurement uncertainties for independent variables are presented in Table 4.

The measurement uncertainty chosen for burn time (the difference between initial and final action times) was set at a level higher than the instrument resolution to account for conceptual bias. Because burn time has a large impact on the calculation of the regression rate, an uncertainty study was conducted to determine the impact of test duration on the calculated uncertainty of the regression rate. Figure 3 shows the effect of decreased testing time as it impacts regression rate uncertainty.

Results and Discussion

Table 5 shows the average oxygen flux, average chamber pressure, and average burning rate with their associated measurement uncertainty for each experiment. The desired pressures and flux levels for each test were generally achieved. Average oxidizer flux varied from 0.095 to 0.109 lbm/in.^{2}-s for tests targeting 0.1 lbm/in.^{2}-s, while those targeting 0.4 lbm/in.^{2}-s oxidizer flux ranged from 0.370 to 0.431 lbm/in.^{2}-s. At high $\bar{G}_{ox}$, chamber pressures achieved during testing ranged from 162 to 190 psi which was slightly lower than the targeted value of 250 psi. One test under high $\bar{G}_{ox}$ conditions resulted in an elevated chamber pressure of 565 psi due to nozzle sizing.

Representative pressure-time curves are shown in Figs. 4–6. These results are for propellant B. The figures show that the tests ignite smoothly and have a fairly neutral pressure-time curve. There were some oscillations in the pressure levels after the chamber filled for both low G_{ox} tests. The exact frequency of the oscillations is difficult to determine because of the low sampling rate (100–1000 Hz) of the data acquisition system. The magnitude of the oscillation in Fig. 6 is about 6% of the mean pressure. The drop of the pressure curves correlates with the shutoff of the main oxygen valve. The decay rate after that point is dependent on the characteristic length of the motor. Just examining the data and assuming an exponential decay after burnout, the time constants for the blowdown range from 0.02 s (high G_{ox}, low pressure), 0.08 s (low G_{ox}, low pressure), to 0.14 s (low G_{ox}, high pressure). With this scheme it takes about two time constants to reach 50% of the pressure that started the blowdown.

Values of average chamber pressure and $\bar{G}_{ox}$ are correlated to the respective burning rates of the different formulations. The three

Table 5 Experimental operating conditions and regression rates

Propellant mix	G_{ox}, lbm/s/in.^{2}	P, psi	$\bar{\dot{r}}$, in./s
A	0.102 ± 8.0%	262 ± 0.4%	0.045 ± 5.7%
A	0.105 ± 8.1%	559 ± 0.2%	0.053 ± 6.4%
A	0.397 ± 7.6%	171 ± 0.6%	0.050 ± 8.7%
B	0.097 ± 8.8%	290 ± 0.4%	0.111 ± 7.8%
B	0.095 ± 8.9%	593 ± 0.2%	0.125 ± 8.6%
B	0.394 ± 8.0%	191 ± 0.5%	0.112 ± 12.5%
C	0.095 ± 8.9%	299 ± 0.4%	0.128 ± 8.7%
C	0.096 ± 8.8%	600 ± 0.2%	0.137 ± 9.8%
C	0.379 ± 6.2%	183 ± 0.6%	0.175 ± 17.4%
D	0.108 ± 7.8%	273 ± 0.4%	0.046 ± 5.6%
D	0.106 ± 8.0%	560 ± 0.2%	0.053 ± 4.8%
D	0.400 ± 8.3%	565 ± 0.2%	0.084 ± 3.9%
E	0.109 ± 8.3%	290 ± 0.4%	0.047 ± 4.0%
E	0.106 ± 8.5%	699 ± 0.2%	0.057 ± 3.8%
E	0.431 ± 7.4%	163 ± 0.6%	0.062 ± 7.8%
F	0.103 ± 8.7%	324 ± 0.3%	0.064 ± 3.3%
F	0.105 ± 8.4%	592 ± 0.2%	0.072 ± 3.6%
F	0.370 ± 8.5%	186 ± 0.5%	0.097 ± 3.3%

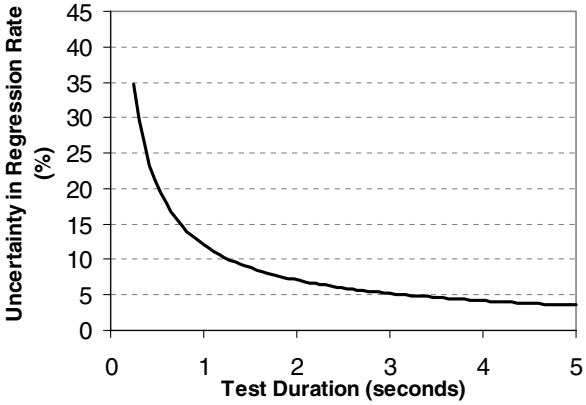

Fig. 3 Uncertainty in regression rate as a function of test time.

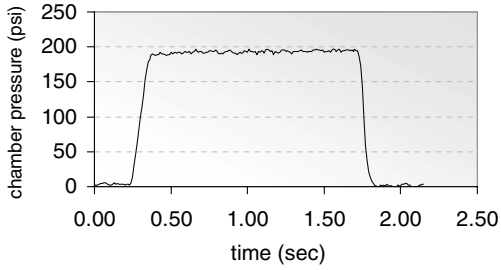

Fig. 4 Propellant B: high G_{ox}, low pressure.

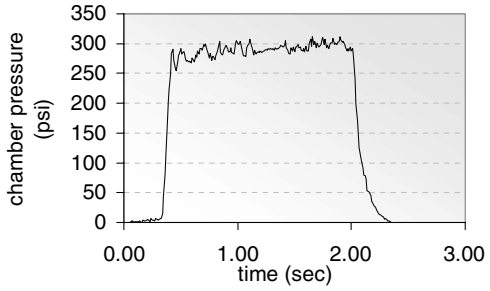

Fig. 5 Propellant B: low G_{ox}, low pressure.

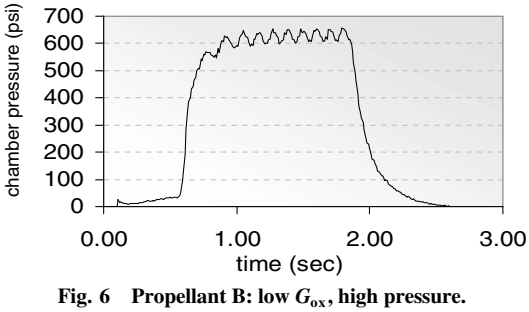

Fig. 6 Propellant B: low G_{ox}, high pressure.

Table 6 Summary of experimental regression rate law parameters

Propellant mix	a	m	n
A	0.019	0.144	0.211
B	0.049	0.057	0.168
C	0.138	0.259	0.093
D	0.031	0.345	0.206
E	0.025	0.297	0.229
F	0.044	0.389	0.214
HTPB	0.051	0.331	0.022

unknown parameters in Eq. (1) were determined from the three sets of operating conditions used for each mixture. A linearized form of Eq. (1) is found by taking the natural log of both sides of the equation. Regression rate coefficients, flux exponents, and pressure exponents for each propellant are given in Table 6.

With a burning rate equation now determined, the results were interpolated to reference conditions and plotted for comparison. Regression rates for mixed hybrid grains operating at 350 psi chamber pressure and an oxidizer flux of 0.3 lbm/in.^{2}-s are shown in Fig. 7. The pure HTPB fuel at an oxidizer flux of 0.3 lbm/in.^{2}-s and an operating pressure of 350 psi has a regression rate of 0.039 in./s. This compares to a value of 0.046 in./s as calculated using an expression given by Sutton [10].

By choosing a representative chamber pressure and oxidizer flux, the relative regression rates of the different fuel mixtures can be compared using the values presented in Table 6 and Eq. (1). A general trend in increased regression rate is noticed with increasing levels of AP and catalyst addition. The highest regression rate noted during testing occurred during the firing of propellant mix C under high $\bar{G}_{ox}$, low pressure conditions. These trends were also apparent when regression rates were calculated for a value of $\bar{G}_{ox}$ equal to 0.1 lbm/in.^{2}-s at pressures of 200 and 500 psi.

When uncertainties are considered, there are three general levels of improvement in regression rates that are apparent in Fig. 7 at the referenced conditions. As AP is added to the grain (mix A, D, and E), regression rates increase from 141% to 176% of pure HTPB. Incorporation of the catalyst with 25% AP (mix B and F) rate increases from 248 to 314% of HTPB. The highest regression rate was realized at a larger constituent of AP (27.5%) with 2.5% catalyst present (mix C) at 447% of HTPB. All uncertainty bands between these three categories of performance did not overlap, indicating that a significant difference in regression rates was present between these three groups of formulations. The values of the mixed hybrid regression rate compared to pure HTPB are provided in standardized form in Table 7.

Experimentation conducted with formulation C (27.5% AP with 2.5% catalyst) exhibited the highest burning rate under all three testing conditions. Uncertainty for testing of this mixture was generally higher than for other formulations, especially at high

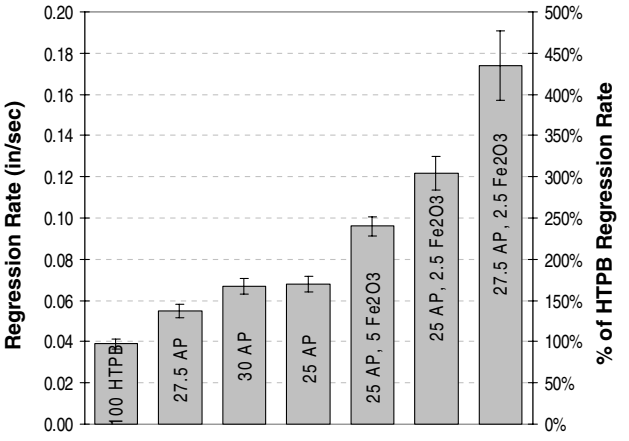

Fig. 7 Mixed hybrid regression rates for $G_{ox} = 0.3$ lbm/in.^{2}-s and $P = 350$ psi.

Table 7 Standardized regression rates for $G_{ox} = 0.3$ lbm/in.^{2}-s and $P = 350$ psi

Propellant mix	$\bar{r}$, in./s	Regression rate ratio
HTPB	0.039	100%
A	0.055	141%
B	0.122	314%
C	0.174	447%
D	0.068	176%
E	0.067	172%
F	0.096	248%

oxidizer flux levels. This is due in part to the reduced burn time required to prevent complete exhaustion of the fuel web.

Using Eq. (1), the regression rate can be plotted as a function of either pressure or oxidizer flux over the operating range considered. Regression rates for propellant mixtures A, B, and C are plotted as a function of G_{ox} at both 250 and 500 psi in Fig. 5. Curves for HTPB are also given at 250 and 500 psi for comparison. The trends observed from Fig. 7 are again present in Fig. 8. Addition of 27.5% AP to the fuel grain (mixture A) results in a small improvement in regression rate over pure HTPB. When a low level of catalyst (2.5%) is added to 25% AP (mixture B), an additional improvement in regression rate is evident. Mixture C contains 27.5% AP with 2.5% catalyst and results in the highest regression rate, as much as 447% of pure HTPB.

Low frequency combustion instability was noted for tests operating under high pressure conditions. Additionally, some residual smoking occurred after oxygen termination when operating at low pressure and flux levels for all grains that contained catalyst. This smoking phenomenon is possibly due to the increased thickness of the thermal layer developed under low pressure operating conditions. Longer burn times were used at low pressures, which allow for a greater abundance of thermal energy to be stored in the fuel grain during the burn.

Because experimental determination of any potential mass loss occurring during the smoking period is included in the determination of the burning rate, a sensitivity study was performed to determine what impact an incremental mass loss due to smoking would cause on the calculated regression rate. Mass losses up to 15 g were considered with no significant impact on the regression rate. Additionally, the chamber pressure measured during the smoking period was virtually zero, which supports the notion of a negligible amount of mass loss.

Conclusions

The experimental determination of regression rate laws for these formulations shows that a mixed hybrid concept using AP and ferric oxide catalyst with gaseous oxygen provides significant augmentation in the solid regression rate. The additives produced pressure sensitivity with exponents from 0.093 to 0.229 and flux exponents ranging from 0.057 to 0.389. Comparison of baseline HTPB tests with literature values suggest good agreement. The additives augment the regression rate of the solid portion of the

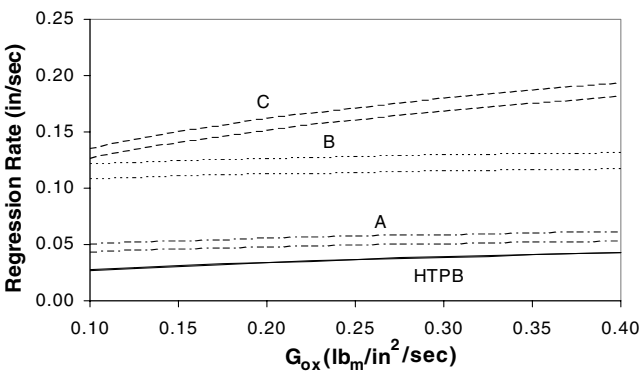

Fig. 8 Regression rate estimates vs G_{ox} with $P = 250$ psi and 500 psi.

mixed hybrid propellant at three general levels. When AP is added, an initial increase in regression rate to a level of 141–176% that of pure HTPB when the results are interpolated to 0.3 lbm/in.^{2}-s and 350 psi. When catalyst is added to grains containing 25% AP, regression rates are further increased to approximately 248–314% the rate of an HTPB grain. The highest level of AP (27.5%) combined with catalyst (2.5%) yielded the highest regression rate augmentation at 447%. Under the conditions tested in this study, all formulations extinguished (with minor residual smoking) when the gaseous oxidizer flow was stopped.

Acknowledgments

This work was sponsored by the Space and Missile Defense Command (SMDC), NASA Marshall Space Flight Center, and the U.S. Army Aviation and Missile Command. The contract was administered by SMDC with Gisele Wilson as the Technical Monitor. United Technologies Chemical Systems Division provided the motor hardware used during testing. The authors acknowledge the assistance of several colleagues on this project. The propellant grains were cast by the U.S. Aviation and Missile, Research, Development, and Engineering Center. Charles L. Martin of NASA Marshall Space Flight Center designed the mixture study.

References

[1] "A Short Course on Concepts, Systems, Applications, and Operating Principles of Hybrid Rockets," AIAA Hybrid Rocket Technical Committee, Washington, D. C., July 1995.

[2] George, P., Krishnan, S., Varkey, P. M., Ravidran, M., and Ramachandran, L., "Fuel Regression Rate in Hydroxyl-Terminated-Polybutadiene Gaseous-Oxygen Hybrid Rocket Motors," *Journal of Propulsion and Power*, Vol. 17, No. 1, Jan.–Feb. 2001, pp. 35–42.

[3] Chiaverini, M. J., Serin, N., Johnson, D. K., Lu, Y., Kuo, K. K., and Risha, G. A., "Regression Rate Behavior of Hybrid Rocket Solid Fuels," *Journal of Propulsion and Power*, Vol. 16, No. 1, Jan.–Feb. 2000, pp. 125–132.

[4] De Zilwa, S., Zilliac, G., Reinath, M., and Karabeyoglu, A., "Time-Resolved Fuel-Grain Port Diameter Measurement in Hybrid Rockets," *Journal of Propulsion and Power*, Vol. 20, No. 4, July–Aug. 2004, pp. 684–689.

[5] Frederick, R. A., Jr., Moser, M. D., Knox, L. R., and Whitehead, J. J., "Ballistic Properties of Mixed Hybrid Propellants," AIAA Paper 2004-3824, July 2004.

[6] Frederick, R. A., Jr., Whitehead, J. J., Knox, L. R., and Moser, M. D., "Regression Rate Study of Mixed Hybrid Propellants," AIAA Paper 2005-3545, July 2005.

[7] Karabeyoglu, A., and Cantwell, B., "Development of Scalable Space-Time Averaged Regression Rate Expressions for Hybrid Rockets," AIAA Paper 2005-3544, 2005.

[8] Coleman, H. W., and Steele, W. G., *Experimentation and Uncertainty Analysis for Engineers*, Wiley, New York, 1999.

[9] Frederick, R. A., and Greiner, B. E., "Laboratory-Scale Hybrid Rocket Motor Uncertainty Analysis," *Journal of Propulsion and Power*, Vol. 12, No. 3, May–June 1996, pp. 605–611.

[10] Sutton, G. P., and Biblarz, O., *Rocket Propulsion Elements*, 7th ed., Wiley, New York, 2001, pp. 590–591.

M. Brewster
Associate Editor